ФИЗИКА ЭЛЕМЕНТАРНЫХ ЧАСТИЦ И АТОМНОГО ЯДРА
2010. Т. 41. ВЫП. 6

# LOW-ENERGY PROPERTIES OF HADRONS IN THE RELATIVISTIC QUARK MODEL

*D. Ebert*[1], *R. N. Faustov*[2], *V. O. Galkin*[2]

[1]Institut für Physik, Humboldt-Universität zu Berlin, Berlin

[2]Dorodnicyn Computing Centre, Russian Academy of Sciences, Moscow

The properties of light and heavy mesons, baryons and tetraquarks are discussed within a QCD-motivated relativistic quark model. The results for the mass spectra, electroweak properties and Regge trajectories of hadrons are presented.

PACS: 12.39.-x

N. N. Bogoliubov always carried out investigations at the frontiers of theoretical and mathematical physics. The quark model of hadrons was proposed by M. Gell-Mann and G. Zweig in 1964. Already in 1965–1966 N. N. Bogoliubov gave lectures on quark model at Moscow State University.

Following Bogoliubov's contribution to the quark pattern of hadrons, we developed the relativistic quark model [1–14]. The model is based on the quasipotential approach in quantum field theory with the QCD-motivated interaction. Hadrons are considered as the bound states of constituent quarks and are described by the single-time wave functions satisfying the three-dimensional Schrödinger-like equation, which is relativistically invariant. The interaction quasi-potential consists of the perturbative one-gluon exchange part and the nonperturbative confining part. The Lorentz structure of the latter part includes the scalar and vector linearly rising interactions. The long-range vector vertex contains the Pauli term (anomalous chromomagnetic quark moment) which enables vanishing of the spin-dependent chromomagnetic interaction in accord with the flux tube model.

Initially the model was formulated for the hadrons containing heavy $c$ and $b$ quarks: charmonium, bottomonium, $B_c$ meson [4], heavy $D$ and $B$ mesons [2], heavy baryons [5, 11] with both one and two heavy quarks. For heavy quarks the physically justified expansion in $v/c$ or the inverse mass of the heavy quark was employed which significantly simplifies calculations. In such calculations we took into account both spin-dependent and spin-independent contributions [2, 4], contrary to most of the previous quark model calculations where spin-independent relativistic corrections were unjustifiably discarded. Mass spectra and electroweak decay rates of heavy quarkonia [4], heavy mesons [3] and heavy baryons [5, 9] were calculated in good agreement with experimental data. Heavy and doubly heavy baryons were treated in the heavy quark–light diquark and light quark–heavy diquark pictures, respectively. The model was also applied to studying exotic charmonium-like states discovered by BaBar, Belle, CDF and CLEO collaborations. These states were treated as tetraquark systems in the diquark–antidiquark picture. The found tetraquark mass spectra [7, 12] are in accord with experimental data.

Many predictions of our model were later confirmed experimentally. Let us mention some of them in the heavy quark sector. In paper [4] we predicted the $B_c$-meson ground state mass $M_{B_c}^{\rm theor} = 6270$ MeV which is in an excellent agreement with the recent experimental value $M_{B_c}^{\rm exp} = (6275.2 \pm 4.3 \pm 2.3)$ MeV (CDF 2006). Our predictions [2] for the masses of the orbitally excited $B_s$-meson states $M_{B_{s2}^*}^{\rm theor} = 5844$ MeV and $M_{B_{s1}}^{\rm theor} = 5831$ MeV were recently confirmed experimentally: $M_{B_{s2}^*}^{\rm exp} = (5839.64 \pm 0.39 \pm 0.14 \pm 0.5)$ MeV and $M_{B_{s1}}^{\rm exp} = (5829.41 \pm 0.2 \pm 0.14 \pm 0.6)$ MeV (CDF 2006). The predicted mass and radiative decay branching fractions [4]: $M_{\eta_b}^{\rm theor} = 9400$ MeV and ${\rm Br}\,(\Upsilon(3S) \to \eta_b\gamma) = 5.1 \cdot 10^{-4}$, ${\rm Br}\,(\Upsilon(2S) \to \eta_b\gamma) = 2.1 \cdot 10^{-4}$ are in good agreement with the very recent measurement: $M_{\eta_b}^{\rm exp} = (9390.4 \pm 3.1)$ MeV and ${\rm Br}\,(\Upsilon(3S) \to \eta_b\gamma) = (4.8 \pm 0.5 \pm 1.2) \cdot 10^{-4}$, ${\rm Br}\,(\Upsilon(2S) \to \eta_b\gamma) = (4.2^{+1.1}_{-1.0} \pm 0.9) \cdot 10^{-4}$ (BaBar 2008, CLEO 2009). As an example, our results for the masses of the ground-state heavy baryons are given in Table 1 in comparison with different theoretical predictions and experimental data. It is clearly seen that there is a good overall agreement with experiment. Our predictions for the masses of $\Omega_c^*$, $\Sigma_b$, $\Sigma_b^*$, $\Xi_b$ and $\Omega_b$, which were obtained in [5], are confirmed by the recent observations of BaBar, CDF and D0 collaborations.

Recently the model has been extended to the description of light mesons and diquarks [6, 13, 14]. The light quarks in our model are treated fully relativistically without application of the inappropriate expansion in $v/c$ $(p/m_q)$. Such a relativistic approach requires to solve a complicated differential Schrödinger-like equation with a potential which depends in a nonlinear way on the mass of the bound state [6]. For this purpose, original numerical methods for the solution of the corresponding quasi-potential equation were developed. The calculated masses of light unflavoured and strange mesons [13] are given in Tables 2 and 3, while the masses of the ground states of light tetraquarks considered as light diquark–antidiquark bound systems [14] are given in Table 4. They are confronted with available experimental data from PDG. We find good agreement of our predictions with data. Most of the well-established state masses are reproduced in our model. The relativistic treatment of the light quark dynamics resulted in a complicated nonlinear dependence of the quark interaction potential on the meson mass. This allowed us to get $\pi$- and $K$-meson masses in agreement with data in our model where chiral symmetry is explicitly broken by the constituent quark masses.

*Table* 1. **Masses of ground-state heavy baryons (in MeV)**

| Baryon | $I(J^P)$ | Theory | | | | | Experiment PDG |
|---|---|---|---|---|---|---|---|
| | | RQM [5] | Roncaglia et al. | Karliner et al. | Jenkins | Lewis, Woloshyn | |
| $\Lambda_c$ | $0(1/2^+)$ | 2297 | 2285 | | | | 2286.46(14) |
| $\Sigma_c$ | $1(1/2^+)$ | 2439 | 2453 | | | | 2453.76(18) |
| $\Sigma_c^*$ | $1(3/2^+)$ | 2518 | 2520 | | | | 2518.0(5) |
| $\Xi_c$ | $1/2(1/2^+)$ | 2481 | 2468 | | | | 2471.0(4) |
| $\Xi_c'$ | $1/2(1/2^+)$ | 2578 | 2580 | | 2580.8(2.1) | | 2578.0(2.9) |
| $\Xi_c^*$ | $1/2(3/2^+)$ | 2654 | 2650 | | | | 2646.1(1.2) |
| $\Omega_c$ | $0(1/2^+)$ | 2698 | 2710 | | | | 2697.5(2.6) |
| $\Omega_c^*$ | $0(3/2^+)$ | 2768 | 2770 | | 2760.5(4.9) | | 2768.3(3.0) (BaBar 2006) |
| $\Lambda_b$ | $0(1/2^+)$ | 5622 | 5620 | | | $5628(^{23}_{50})$ | 5620.2(1.6) |
| $\Sigma_b$ | $1(1/2^+)$ | 5805 | 5820 | 5814 | 5824.2(9.0) | $5793(^{17}_{21})$ | 5807.5(2.5) (CDF 2006 ($\Sigma_b^+$)) |
| $\Sigma_b^*$ | $1(3/2^+)$ | 5834 | 5850 | 5836 | 5840.0(8.8) | $5814(^{26}_{27})$ | 5829.0(2.3) (CDF 2006 ($\Sigma_b^+$)) |
| $\Xi_b$ | $1/2(1/2^+)$ | 5812 | 5810 | 5795(5) | 5805.7(8.1) | $5755(^{18}_{23})$ | 5792.9(3.0) (CDF 2007) |
| $\Xi_b'$ | $1/2(1/2^+)$ | 5937 | 5950 | 5930(5) | 5950.9(8.5) | $5885(^{15}_{18})$ | |
| $\Xi_b^*$ | $1/2(3/2^+)$ | 5963 | 5980 | 5959(4) | 5966.1(8.3) | $5897(^{40}_{25})$ | |
| $\Omega_b$ | $0(1/2^+)$ | 6065 | 6060 | 6052(6) | 6068.7(11.1) | $6001(^{12}_{19})$ | 6054.4(6.8) (D0 2008); 6165(23) (CDF 2009) |
| $\Omega_b^*$ | $0(3/2^+)$ | 6088 | 6090 | 6083(6) | 6083.2(11.0) | $6013(^{18}_{23})$ | |

The scalar sector presents a special interest due to its complexity and the abundance of experimentally observed light states. We see from Table 2 that the masses of the lightest $q\bar{q}$ scalar mesons have values about 1200 MeV. On the other hand, the results presented in Table 4 indicate that light scalar mesons, $f_0(600)$ $(\sigma)$, $K_0^*(800)$, $f_0(980)$ and $a_0(980)$, with masses below 1 GeV should be described as light tetraquarks consisting of scalar diquark and antidiquark. The predicted masses of the scalar tetraquarks composed of axial-vector diquark and antidiquark have masses in the same range as the lowest $q\bar{q}$ scalar mesons. The obtained results for the masses indicate that $a_0(1450)$ should be predominantly a tetraquark state which predicted mass 1480 MeV is within experimental error bars $M_{a_0(1450)} = (1474 \pm 19)$ MeV. The exotic scalar state $X(1420)$ from the «Further States» Section could be its isotensor partner. On the other hand, the $s\bar{q}(1^3P_0)$ interpretation is favored for $K_0^*(1430)$ (see Table 3). This picture naturally explains the experimentally observed proximity of masses of the unflavoured $a_0(1450)$ and $f_0(1500)$ with the strange $K_0^*(1430)$. Therefore, one could expect an additional isovector predominantly $q\bar{q}$ state $a_0$ with the mass about 1200 MeV, though it was not observed in several experiments.

*Table* 2. **Masses of excited light ($q = u, d$) unflavored mesons (in MeV)**

| State | $J^{PC}$ | Theory | Experiment | | | | Theory | Experiment | |
|---|---|---|---|---|---|---|---|---|---|
| | | $q\bar{q}$ | $I=1$ | Mass | $I=0$ | Mass | $s\bar{s}$ | $I=0$ | Mass |
| $1^1S_0$ | $0^{-+}$ | 154 | $\pi$ | 139.57 | | | 743 | | |
| $1^3S_1$ | $1^{--}$ | 776 | $\rho$ | 775.49(34) | $\omega$ | 782.65(12) | 1038 | $\varphi$ | 1019.455 |
| $1^3P_0$ | $0^{++}$ | 1176 | $a_0$ | 1474(19) | $f_0$ | 1200-1500 | 1420 | $f_0$ | 1505(6) |
| $1^3P_1$ | $1^{++}$ | 1254 | $a_1$ | 1230(40) | $f_1$ | 1281.8(6) | 1464 | $f_1$ | 1426.4(9) |
| $1^3P_2$ | $2^{++}$ | 1317 | $a_2$ | 1318.3(6) | $f_2$ | 1275.1(12) | 1529 | $f_2'$ | 1525(5) |
| $1^1P_1$ | $1^{+-}$ | 1258 | $b_1$ | 1229.5(32) | $h_1$ | 1170(20) | 1485 | $h_1$ | 1386(19) |
| $2^1S_0$ | $0^{-+}$ | 1292 | $\pi$ | 1300(100) | $\eta$ | 1294(4) | 1536 | $\eta$ | 1476(4) |
| $2^3S_1$ | $1^{--}$ | 1486 | $\rho$ | 1465(25) | $\omega$ | 1400-1450 | 1698 | $\varphi$ | 1680(20) |
| $1^3D_1$ | $1^{--}$ | 1557 | $\rho$ | 1570(70) | $\omega$ | 1670(30) | 1845 | | |
| $1^3D_2$ | $2^{--}$ | 1661 | | | | | 1908 | | |
| $1^3D_3$ | $3^{--}$ | 1714 | $\rho_3$ | 1688.8(21) | $\omega_3$ | 1667(4) | 1950 | $\varphi_3$ | 1854(7) |
| $1^1D_2$ | $2^{-+}$ | 1643 | $\pi_2$ | 1672.4(32) | $\eta_2$ | 1617(5) | 1909 | $\eta_2$ | 1842(8) |
| $2^3P_0$ | $0^{++}$ | 1679 | | | $f_0$ | 1724(7) | 1969 | | |
| $2^3P_1$ | $1^{++}$ | 1742 | $a_1$ | 1647(22) | | | 2016 | $f_1$ | 1971(15) |
| $2^3P_2$ | $2^{++}$ | 1779 | $a_2$ | 1732(16) | $f_2$ | 1755(10) | 2030 | $f_2$ | 2010(70) |
| $2^1P_1$ | $1^{+-}$ | 1721 | | | | | 2024 | | |
| $3^1S_0$ | $0^{-+}$ | 1788 | $\pi$ | 1816(14) | $\eta$ | 1756(9) | 2085 | $\eta$ | 2103(50) |
| $3^3S_1$ | $1^{--}$ | 1921 | $\rho$ | 1909(31) | $\omega$ | 1960(25) | 2119 | $\varphi$ | 2175(15) |
| $1^3F_2$ | $2^{++}$ | 1797 | | | $f_2$ | 1815(12) | 2143 | $f_2$ | 2156(11) |
| $1^3F_3$ | $3^{++}$ | 1910 | $a_3$ | 1874(105) | | | 2215 | $f_3$ | 2334(25) |
| $1^3F_4$ | $4^{++}$ | 2018 | $a_4$ | 2001(10) | $f_4$ | 2018(11) | 2286 | | |
| $1^1F_3$ | $3^{+-}$ | 1884 | | | | | 2209 | $h_3$ | 2275(25) |

*Table* 3. **Masses of strange mesons (in MeV)**

| State | $J^P$ | Theory | Experiment | |
|---|---|---|---|---|
| | | $q\bar{s}$ | $I=1/2$ | Mass |
| $1^1S_0$ | $0^-$ | 482 | $K$ | 493.677(16) |
| $1^3S_1$ | $1^-$ | 897 | $K^*$ | 891.66(26) |
| $1^3P_0$ | $0^+$ | 1362 | $K_0$ | 1425(50) |
| $1^3P_2$ | $2^+$ | 1424 | $K_2^*$ | 1425.6(15) |
| $1P_1$ | $1^+$ | 1412 | $K_1$ | 1403(7) |
| $1P_1$ | $1^+$ | 1294 | $K_1$ | 1272(7) |
| $2^1S_0$ | $0^-$ | 1538 | | |
| $2^3S_1$ | $1^-$ | 1675 | $K^*$ | |
| $1^3D_1$ | $1^-$ | 1699 | $K^*$ | 1717(27) |
| $1^3D_3$ | $3^-$ | 1789 | $K_3^*$ | 1776(7) |
| $1D_2$ | $2^-$ | 1824 | $K_2$ | 1816(13) |
| $1D_2$ | $2^-$ | 1709 | $K_2$ | 1773(8) |
| $2^3P_0$ | $0^+$ | 1791 | | |
| $2^3P_2$ | $2^+$ | 1896 | | |
| $2P_1$ | $1^+$ | 1893 | | |
| $2P_1$ | $1^+$ | 1757 | $K_1$ | 1650(50) |

*Table* 4. **Masses of light tetraquark ground state ($\langle \mathbf{L}^2 \rangle = 0$) (in MeV) and possible experimental candidates. $S$ and $A$ denote scalar and axial vector diquarks**

| State | Diquark | Theory | Experiment | | | |
|---|---|---|---|---|---|---|
| $J^{PC}$ | content | mass | $I=0$ | Mass | $I=1$ | Mass |
| $(qq)(\bar{q}\bar{q})$ | | | | | | |
| $0^{++}$ | $S\bar{S}$ | 596 | $f_0(600)$ $[\sigma]$ | 400–1200 | | - |
| $1^{+\pm}$ | $(S\bar{A} \pm \bar{S}A)/\sqrt{2}$ | 672 | | | | |
| $0^{++}$ | $A\bar{A}$ | 1179 | $f_0(1370)$ | 1200–1500 | | |
| $1^{+-}$ | $A\bar{A}$ | 1773 | | | | |
| $2^{++}$ | $A\bar{A}$ | 1915 | $f_2(1910)$ | 1903(9) | | |
| | | | $f_2(1950)$ | 1944(12) | | |
| $(qs)(\bar{q}\bar{s})$ | | | | | | |
| $0^{++}$ | $S\bar{S}$ | 992 | $f_0(980)$ | 980(10) | $a_0(980)$ | 984.7(12) |
| $1^{++}$ | $(S\bar{A} + \bar{S}A)/\sqrt{2}$ | 1201 | $f_1(1285)$ | 1281.8(6) | $a_1(1260)$ | 1230(40) |
| $1^{+-}$ | $(S\bar{A} - \bar{S}A)/\sqrt{2}$ | 1201 | $h_1(1170)$ | 1170(20) | $b_1(1235)$ | 1229.5(32) |
| $0^{++}$ | $A\bar{A}$ | 1480 | $f_0(1500)$ | 1505(6) | $a_0(1450)$ | 1474(19) |
| $1^{+-}$ | $A\bar{A}$ | 1942 | $h_1(1965)$ | 1965(45) | $b_1(1960)$ | 1960(35) |
| $2^{++}$ | $A\bar{A}$ | 2097 | $f_2(2010)$ | 2011(70) | $a_2(1990)$ | 2050(45) |
| | | | $f_2(2140)$ | 2141(12) | $a_2(2080)$ | 2100(20) |
| $(ss)(\bar{s}\bar{s})$ | | | | | | |
| $0^{++}$ | $A\bar{A}$ | 2203 | $f_0(2200)$ | 2189(13) | | — |
| $1^{+-}$ | $A\bar{A}$ | 2267 | $h_1(2215)$ | 2215(40) | | — |
| $2^{++}$ | $A\bar{A}$ | 2357 | $f_2(2340)$ | 2339(60) | | — |
| | | | $I=1/2$ | | — | — |
| $(qq)(\bar{s}\bar{q})$ | | | | | | |
| $0^{+}$ | $S\bar{S}$ | 730 | $K_0^*(800)$ $(\kappa)$ | 672(40) | | |
| $1^{+}$ | $(S\bar{A} \pm \bar{S}A)/\sqrt{2}$ | 1057 | | | | |
| $0^{+}$ | $A\bar{A}$ | 1332 | $K_0^*(1430)$ | 1425(50) | | |
| $1^{+}$ | $A\bar{A}$ | 1855 | | | | |
| $2^{+}$ | $A\bar{A}$ | 2001 | $K_2^*(1980)$ | 1973(26) | | |

In Figs. 1 and 2 we plot the Regge trajectories in the $(J, M^2)$ plane for mesons with natural ($P = (-1)^J$) and unnatural ($P = (-1)^{J-1}$) parity, respectively. The masses calculated in our model are shown by diamonds. Available experimental data are given by dots with error bars and corresponding meson names. Straight lines were obtained by a $\chi^2$ fit of the calculated values. The corresponding Regge trajectories in the $(n_r, M^2)$ plane can be found in [13]. We see that the calculated light meson masses fit nicely the linear trajectories in both planes. These trajectories are almost parallel and equidistant. It is important to note that the quality of fitting the $\pi$-meson Regge trajectories is being significantly improved if the ground-state $\pi$ is excluded from the fit. In the kaon case omitting the ground state also improves the fit but not so dramatically as for the pion. The corresponding trajectories are shown in Fig. 2 by dashed lines.

New methods for the calculation of the hadronic matrix elements for the electroweak decays with the consistent account of relativistic contributions have

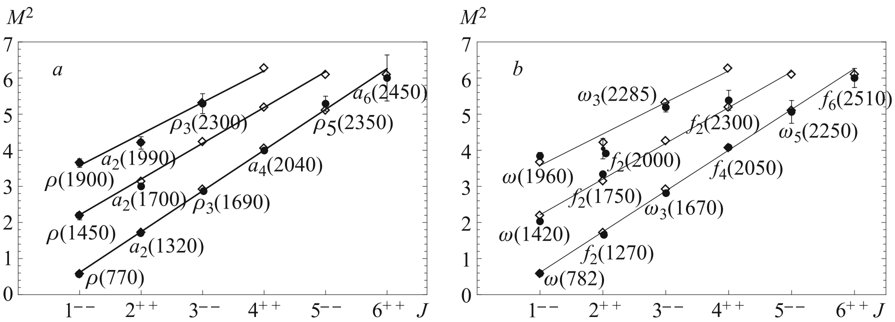


Fig. 1. Parent and daughter $(J, M^2)$ Regge trajectories for isovector (*a*) and isoscalar (*b*) light mesons with natural parity. Diamonds are predicted masses. Available experimental data are given by dots with error bars and particle names. $M^2$ is in $\mathrm{GeV}^2$

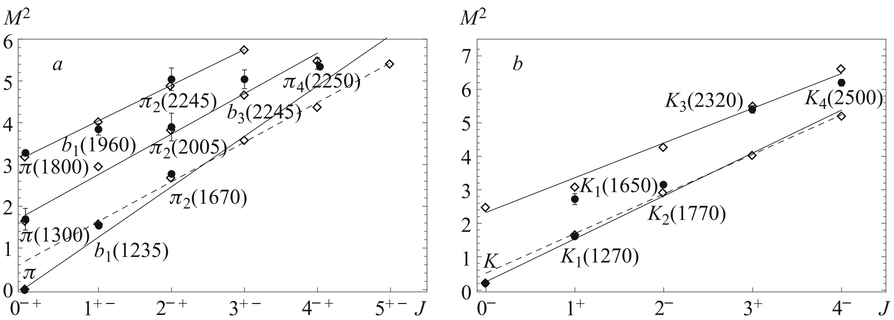


Fig. 2. Parent and daughter $(J, M^2)$ Regge trajectories for isovector (*a*) and isodoublet (*b*) light mesons with unnatural parity. Dashed line corresponds to the Regge trajectory, fitted without $\pi$ and $K$

been developed. Special attention is paid to the recoil effects of the final hadrons and corresponding relativistic transformations of the hadron wave functions from the rest to the moving reference frame, as well as to the relativistic contributions of the intermediate negative-energy states [6, 10]. Application of these methods can be demonstrated with the calculation of the decay constants $f_P$ and $f_V$ of the pseudoscalar ($P$) and vector ($V$) mesons [8]. They are defined by

$$\begin{aligned} \langle 0|\bar{q}_1\gamma^\mu\gamma_5 q_2|P(\mathbf{K})\rangle &= i f_P K^\mu, \\ \langle 0|\bar{q}_1\gamma^\mu q_2|V(\mathbf{K},\varepsilon)\rangle &= f_V M_V \varepsilon^\mu, \end{aligned} \tag{1}$$

where $\mathbf{K}$ is the meson momentum, $\varepsilon^\mu$ and $M_V$ are the polarization vector and mass of the vector meson. These matrix elements can be expressed through the two-particle wave function in the quark loop integral (see Fig. 3)

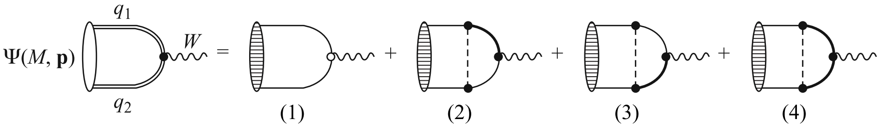


Fig. 3. Weak annihilation diagram of the light meson. Solid and bold lines denote the positive- and negative-energy part of the quark propagator, respectively. Dashed lines represent the interaction operator

$$\begin{aligned}\langle <0|J_\mu^W|M(\mathbf{K})\rangle &= \int \frac{d^3p}{(2\pi)^3}\,\mathrm{Tr}\left\{\gamma_\mu(1-\gamma_5)\Psi(M,\mathbf{p})\right\},\\ \Psi(M,\mathbf{p}) &= \int \frac{dp^0}{2\pi}\Psi(M,p),\end{aligned}\tag{2}$$

$\Psi(M,p)$ is the two-particle Bethe–Salpeter wave function and $\Psi(M,\mathbf{p})$ is the single-time wave function containing both positive- and negative-energy quark states. Since in the quasi-potential approach the wave function is projected onto the positive-energy states, it is necessary to include additional terms which account for the contributions of negative-energy intermediate states. The weak annihilation amplitude (2) is schematically presented in the left-hand side of Fig. 3. The first diagram in the right-hand side corresponds to the simple replacing of the single-time wave function by the quasi-potential one. The second and third diagrams account for negative-energy contributions to the first and second quark propagators, respectively. The last diagram corresponds to negative-energy contributions from both quark propagators. The resulting expression for the decay constant is the following:

$$f_{P,V} = f_{P,V}^{(1)} + f_{P,V}^{(2+3)} + f_{P,V}^{(4)},\tag{3}$$

where the terms in the right-hand side originate from the corresponding diagrams in Fig. 3. Note that the negative-energy contributions $f_{P,V}^{(2+3)}$ and $f_{P,V}^{(4)}$ are new. Their explicit expressions can be found in [8].

In Table 5 we give different contributions to the pseudoscalar and vector decay constants of light and heavy-light mesons. It is clearly seen that the nonrelativistic predictions are significantly overestimating the decay constants, especially for the pion and kaon. The partial account of relativistic corrections by keeping in only the first term $f_M^{(1)}$, which is usually used for semirelativistic calculations, does not substantially improve the situation. The disagreement is still large. This is connected with the anomalously small masses of light pseudoscalar mesons exhibiting their chiral nature. Thus, it is not justified to neglect contributions of the negative-energy intermediate states for light-meson decay constants. Indeed, the values of $f_M^{(2+3)} + f_M^{(4)}$ are large and negative (reaching 76% of $f_\pi^{(1)}$ for the

*Table* 5. **Different contributions to the pseudoscalar and vector decay constants of light and heavy-light mesons (in MeV)**

| Constant | $f_M^{\rm NR}$ | $f_M^{(1)}$ | $f_M^{(2+3)} + f_M^{(4)}$ | $(f_M^{(2+3)} + f_M^{(4)})/f_M^{(1)}$, % | $f_M$ | Exp. |
|---|---|---|---|---|---|---|
| $f_\pi$ | 1290 | 515 | $-391$ | $-76$ | 124 | 130.4(2) |
| $f_\rho$ | 490 | 402 | $-183$ | $-46$ | 219 | 220(2) |
| $f_K$ | 783 | 353 | $-198$ | $-56$ | 155 | 155.5(9) |
| $f_{K^*}$ | 508 | 410 | $-174$ | $-42$ | 236 | 217(5) |
| $f_\phi$ | 511 | 415 | $-170$ | $-41$ | 245 | 229(3) |
| $f_D$ | 376 | 275 | $-41$ | $-15$ | 234 | 208(9) |
| $f_{D^*}$ | 391 | 334 | $-24$ | $-7$ | 310 | |
| $f_{D_s}$ | 436 | 306 | $-38$ | $-12$ | 268 | 269(9) |
| $f_{D_s^*}$ | 447 | 367 | $-52$ | $-14$ | 315 | |
| $f_B$ | 259 | 210 | $-21$ | $-10$ | 189 | 227(52) |
| $f_{B^*}$ | 280 | 235 | $-16$ | $-7$ | 219 | |
| $f_{B_s}$ | 300 | 238 | $-20$ | $-8$ | 218 | |
| $f_{B_s^*}$ | 316 | 264 | $-13$ | $-5$ | 251 | |
| $f_{B_c}$ | 538 | 433 | $-8$ | $-1.8$ | 425 | |
| $f_{B_c^*}$ | 545 | 503 | $-4$ | $-0.8$ | 499 | |

pion) compensating the overestimation of decay constants by the positive-energy contribution $f_M^{(1)}$. Their account brings theoretical predictions in accord with available experimental data.

The same approach can be used for the calculation of the pion electromagnetic form factor in the space-like region [6]. The results of such calculations are shown in Fig. 4 in comparison with experimental data. Good agreement with data in both low- and high-$Q^2$ regions is found. It is seen from Fig. 4 that the calculated pion form factor at high $Q^2$ exhibits the asymptotic behaviour $F_\pi(Q^2) \sim \alpha_s(Q^2)/Q^2$ predicted by the quark counting rule and perturbative QCD.

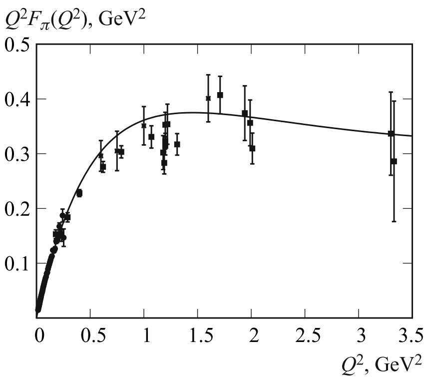


Fig. 4. The product of $Q^2$ and form factor of charged pion in comparison with experimental data

Various other electroweak properties and decays of light and heavy hadrons were considered. It is important to emphasize that our relativistic quark model is completely compatible with the model-independent relations imposed by the heavy quark symmetry [1]. It was checked that these relations for the form factors of the heavy-to-heavy weak transition matrix elements are satisfied in the model at both leading and subleading orders of the heavy-quark expansion [1, 9]. They were tested for the decays to orbitally and radially excited heavy mesons. Therefore, our model provides an explicit determination of the leading and subleading Isgur–Wise functions as overlap integrals of the corresponding meson wave functions [10]. The symmetry relations between form factors of heavy-to-light and rare radiative $B$-meson decays were also studied in the limit of infinitely heavy $b$ quark and large recoil energy of the final light meson [3]. It was shown that the heavy quark and large recoil energy symmetries significantly reduce the number of independent form factors and impose numerous relations among them. It was tested that these relations are satisfied and independent invariant functions were determined.

The small number (ten) of free parameters, the values of which are universal for all considered hadrons (mesons, baryons and tetraquarks), is an important merit of our model. The choice of the specific parameters — the long-range anomalous chromomagnetic quark moment and the mixing parameter of the vector and scalar confining potentials — got additional justification from the heavy-quark symmetry relations in QCD [1,9]. The developed quark model gives a large number (several hundreds) of predictions for masses and decay rates of different hadrons which agree well with available experimental data.

This work was supported in part by the Russian Science Support Foundation (V. O. G.) and the Russian Foundation for Basic Research grant No. 08-02-00582.

## REFERENCES

1. *Faustov R. N., Galkin V. O.* // Z. Phys. C. 1995. V. 66. P. 119.
2. *Ebert D., Galkin V. O., Faustov R. N.* // Phys. Rev. D. 1998. V. 57. P. 5663.
3. *Ebert D., Faustov R. N., Galkin V. O.* // Phys. Rev. D. 2001. V. 64. P. 094022.
4. *Ebert D., Faustov R. N., Galkin V. O.* // Phys. Rev. D. 2003. V. 67. P. 014027.
5. *Ebert D., Faustov R. N., Galkin V. O.* // Phys. Rev. D. 2005. V. 72. P. 034026.
6. *Ebert D., Faustov R. N., Galkin V. O.* // Eur. Phys. J. C. 2006. V. 47. P. 745.
7. *Ebert D., Faustov R. N., Galkin V. O.* // Phys. Lett. B. 2006. V. 634. P. 214.
8. *Ebert D., Faustov R. N., Galkin V. O.* // Ibid. V. 635. P. 93.
9. *Ebert D., Faustov R. N., Galkin V. O.* // Phys. Rev. D. 2006. V. 73. P. 094002.
10. *Ebert D., Faustov R. N., Galkin V. O.* // Phys. Rev. D. 2007. V. 75. P. 074008.
11. *Ebert D., Faustov R. N., Galkin V. O.* // Phys. Lett. B. 2008. V. 659. P. 612.
12. *Ebert D., Faustov R. N., Galkin V. O.* // Eur. Phys. J. C. 2008. V. 58. P. 399.
13. *Ebert D., Faustov R. N., Galkin V. O.* // Phys. Rev. D. 2009. V. 79. P. 114029.
14. *Ebert D., Faustov R. N., Galkin V. O.* // Eur. Phys. J. C. 2009. V. 60. P. 273.